



## Heterogeneous ozone catalytic degradation of butyl xanthate with $\gamma$ -Al<sub>2</sub>O<sub>3</sub> loaded with Pt, Au and Pd

Han Wei<sup>a</sup>, Qiu-rong Long<sup>b</sup>, Wen-bo Dong<sup>a,\*</sup>, Jian-hua Chen<sup>c</sup>, Yu-qiong Li<sup>c</sup>

<sup>a</sup>Department of Environmental Science and Engineering, Fudan University, Shanghai 200433, China, emails: 861382202@qq.com (W.B. Dong), 62503432@qq.com (H. Wei)

<sup>b</sup>Department of Materials Science and Engineering, Southern University of Science and Technology, Shenzhen 518055, China, email: 283447398@qq.com

<sup>c</sup>College of Resources, Environment and Material Science and Engineering, Guangxi University, Nanning 530004, China, emails: jhchen@gxu.edu.cn (J.H. Chen), lyq198205@163.com (Y.Q. Li)

Received 24 February 2018; Accepted 9 April 2018

### ABSTRACT

The Pt-, Au- and Pd-loaded  $\gamma$ -Al<sub>2</sub>O<sub>3</sub> catalysts were prepared by the dipping method, and the effect of the Pt, Au and Pd loading on the performance in the heterogeneous ozone catalytic degradation of xanthate was investigated. The kinetics of the degradation process and the degradation pathways were studied by UV absorption experiments and density function theory calculations. The results show that heterogeneous ozone catalytic degradation of xanthate by Pt-, Au- and Pd-loaded  $\gamma$ -Al<sub>2</sub>O<sub>3</sub> can significantly improve the degradation efficiency, with Pt showing the best performance, followed by Au and Pd. The experimental results show that the mechanism of the catalytic degradation of xanthate by the Pt-, Au- and Pd-loaded  $\gamma$ -Al<sub>2</sub>O<sub>3</sub> catalysts is the oxidation of free radicals. The degradation of xanthate begins from the rupture of the C–S bond, followed by the C–O bond.

**Keywords:** Heterogeneous ozone catalysis;  $\gamma$ -Al<sub>2</sub>O<sub>3</sub>; Noble metal support; Butyl xanthate; Mine wastewater

### 1. Introduction

Most mineral processing reagents used in mines require a large dosage and display the characteristics of high pollution and high toxicity [1]. These chemicals and their decomposition products are largely discharged from mineral processing wastewater and give rise to significant pollution in the environment, attracting much attention to this problem [2]. Hence, the treatment of mine wastewater is very important for environmental protection. Xanthate is one of the most important flotation reagents in the mineral processing industry. Compared with other chemicals, the dosage of xanthate is large, such that the residual amount in mineral processing wastewater is also large, causing severe pollution of the

environment. Therefore, more effective degradation and treatment of wastewater from mineral processing is of great environmental significance.

Catalytic ozonation techniques developed in recent years can effectively degrade organic compounds that are difficult to oxidize by ozone alone under normal temperature and pressure [3]. The homogeneous catalysts are divided into two types, the first consisting of metal ions only, whereas the second type of catalyst is loaded with metal and/or metal oxide [4,5]. Compared with common Al<sub>2</sub>O<sub>3</sub>,  $\gamma$ -Al<sub>2</sub>O<sub>3</sub> has a larger specific surface area, more narrow pore size distribution and larger pore size, enabling better loading of the metal ions and enhancing the performance of the catalyst [6–8].

In this work, the  $\gamma$ -Al<sub>2</sub>O<sub>3</sub> catalysts loaded with Pt, Au and Pd were prepared by the dipping method, and the effects

\* Corresponding author.

Presented at the 3rd International Conference on Recent Advancements in Chemical, Environmental and Energy Engineering, 15–16 February, Chennai, India, 2018.

of Pt, Au and Pd on the degradation of butyl xanthate were studied. The catalytic degradation mechanism and products were investigated using a UV spectrophotometer and density function theory (DFT) calculations. The obtained research results provide deep insight into the thorough purification of mine wastewater.

## 2. Experimental method

### 2.1. Preparation of catalyst

In this experiment, the dipping method was used to prepare the catalyst. The chemical reagents used in the experiment are chloroplatinic acid, chloroauric acid, palladium chloride (industrially pure chloroauric acid obtained from Guoyao Chemical Reagent Co., Ltd., Shanghai, China), butyl xanthate and isobutyl xanthate (industrially pure, laboratory preparation). By dipping  $\gamma\text{-Al}_2\text{O}_3$  in acid solutions with different concentrations of Pt, Au and Pd, the volume of the solution was completely soaked into the powder and the solutions were left to stand for 24 h at room temperature and then dried at 100°C under the vacuum pressure of 0.1 MPa. After drying, the samples were calcined in a muffle furnace, and the calcination temperature was adjusted from room temperature to 400°C and the samples were kept warm for 4 h; the samples were then taken out after cooling to room temperature and were stored in a sealed container.

### 2.2. Experimental procedure

The experiments were carried out in a plastic reactor (15 cm in diameter and 25 cm in length) built in-house, as

shown in Fig. 1. The experiments were conducted at room temperature, and the wastewater samples had the volume of 1.0 L in each experiment. All solutions were configured with distilled water. Prior to each experiment, the ozone generator was checked for normal operation.

The experimental procedure was as follows: first, the ozone generator was checked and the ozone flow rate was adjusted. Second, the butyl xanthate solution was prepared and the catalyst was weighed precisely. Third, the ozone generator was opened and emptied for approximately 3 min until the ozone concentration was stable; then, the butyl xanthate solution and the catalyst were added to the reactor and the ozone gas was flowed into the reactor prior to the reaction.

### 2.3. Computational simulations

In this study, the properties of  $\gamma\text{-Al}_2\text{O}_3$  coated with Au, Pt and Pd metals were studied by DFT calculations using the CASTEP code with the GGA PBE exchange-correlation potentials [9,10]. Only valence electrons were considered explicitly through the use of ultrasoft pseudopotentials [11]. The surfaces were obtained from the relaxed bulk structure. Adsorption studies were performed using surface supercells corresponding to  $(2 \times 2)$  surface unit cells, and a Monkhorst–Pack [12,13]  $k$ -point sampling density of  $3 \times 3 \times 2$  was used for all adsorption calculations. In addition, vacuum with the thickness of 15 Å was placed between the surface slabs. The convergence tolerances for the geometry optimization calculations were set to the maximum displacement of 0.002 Å, the maximum force of 0.05 eV Å<sup>-1</sup>, the maximum energy change of  $2.0 \times 10^{-5}$  eV·atom<sup>-1</sup> and the maximum stress of 0.1 GPa, and the self-consistent field

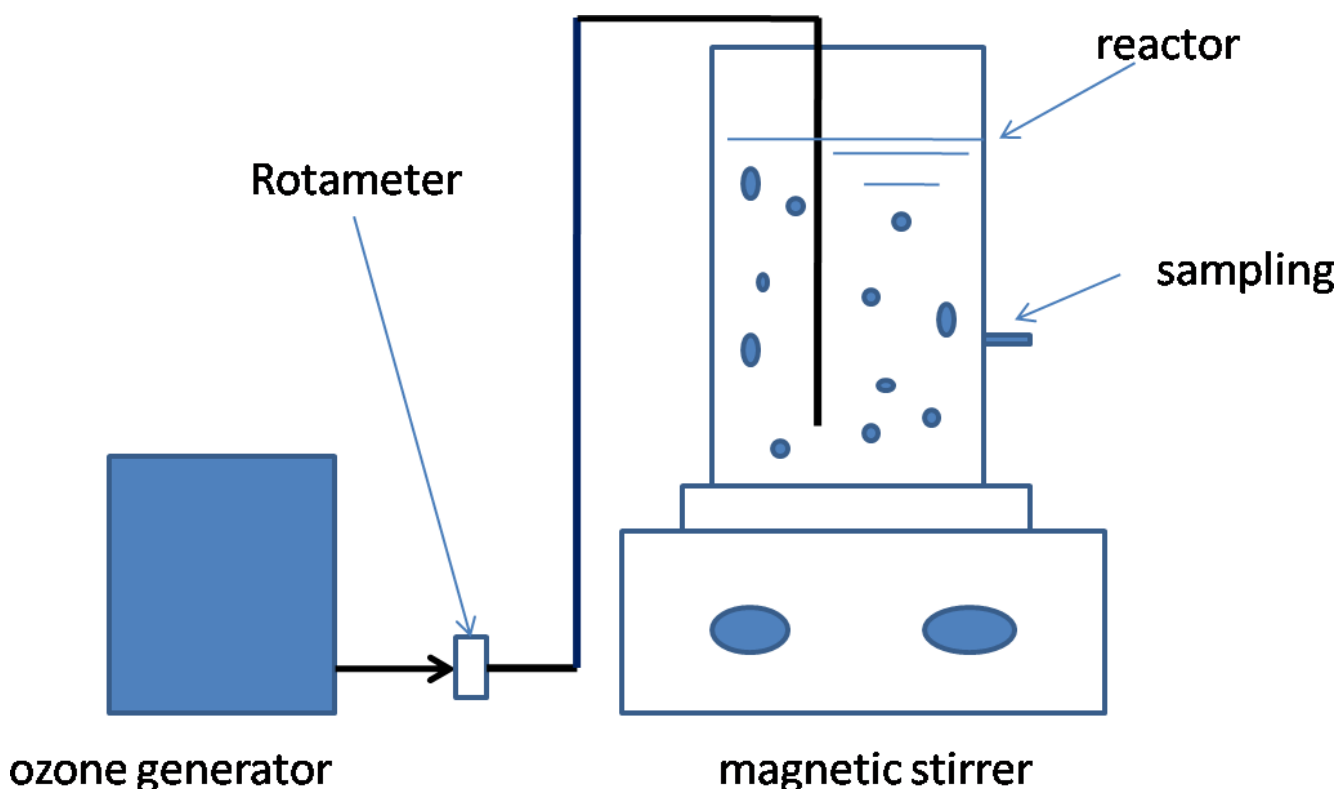


Fig. 1. Experimental graph.

convergence tolerance was set to  $2.0 \times 10^{-6}$  eV atom<sup>-1</sup>. In addition, spin-polarization was used for all calculations.

The optimized molecular structure of xanthate is shown in Fig. 2, and the (101) face of  $\gamma$ -alumina-supported platinum, gold and palladium atoms is shown in Fig. 3.

The adsorption energy of a metal on a surface is defined by [14]:

$$E_{\text{ads}} = E_{\text{metal/slab}} - E_{\text{metal}} - E_{\text{slab}} \quad (1)$$

where  $E_{\text{ads}}$  is the adsorption energy,  $E_{\text{metal/slab}}$  is the total energy after the metal is adsorbed on the surface, and  $E_{\text{metal}}$  and  $E_{\text{slab}}$  are the total energies of the metal and the layer crystal surface prior to the adsorption, respectively. Lower values of the adsorption energy correspond to more stable adsorption. Otherwise, the stability is lower.

### 3. Results and discussion

#### 3.1. Effect of loading concentration on degradation

The Pt, Au and Pd were supported on the  $\gamma$ -Al<sub>2</sub>O<sub>3</sub> by dipping the corresponding metal at the concentrations of 0.01,

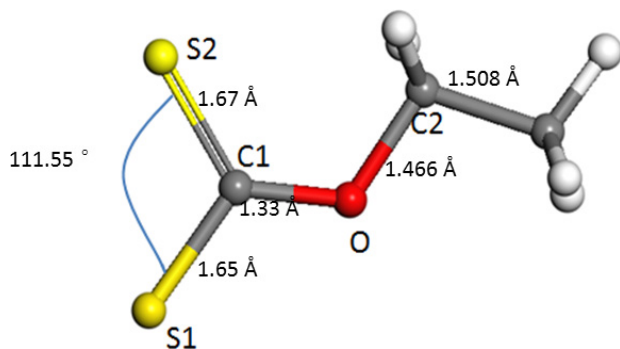


Fig. 2. Configuration of optimized xanthate.

0.02, 0.03, 0.04 and 0.05 mol/L; hence, a higher concentration corresponds to the greater amount of precious metals supported on the surface of the  $\gamma$ -Al<sub>2</sub>O<sub>3</sub>. The effect of different metal concentrations on the oxidation of butyl xanthate is shown in Fig. 4. It can be seen that when the metal loading concentration increased from 0.01 to 0.05 mol/L, the degradation rate first increases and then decreases. The degradation rates of xanthate all reached the highest value when the loading concentration of Pt, Au and Pd was 0.04 mol/L, suggesting that the metal solution concentration of 0.04 mol/L is the optimum dipping concentration. Hence, the dipping concentration of the metal solution was fixed at 0.04 mol/L in the subsequent experiments. The results in Fig. 4 also indicate that the Pt had the best catalytic efficiency, followed by Au and Pd.

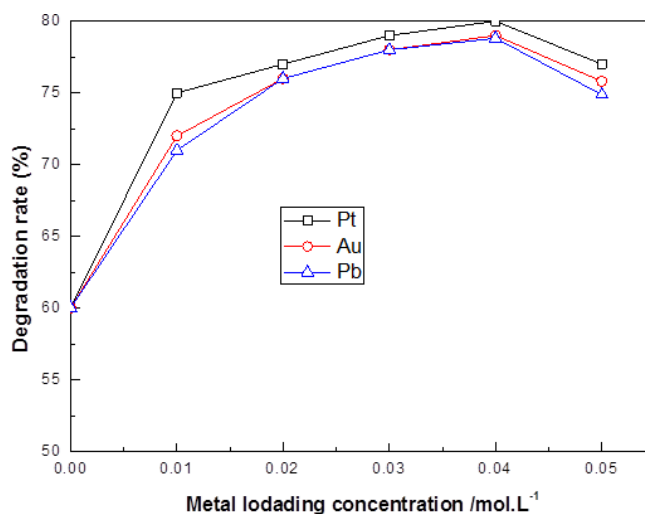


Fig. 4. Relationship between the metal loading concentration and degradation rate of butyl xanthate at the conditions of 100 mg/L initial concentration of butyl xanthate, 0.5 g/L addition of catalyst, 1.75 g/h ozone flow and 5 min degradation time.

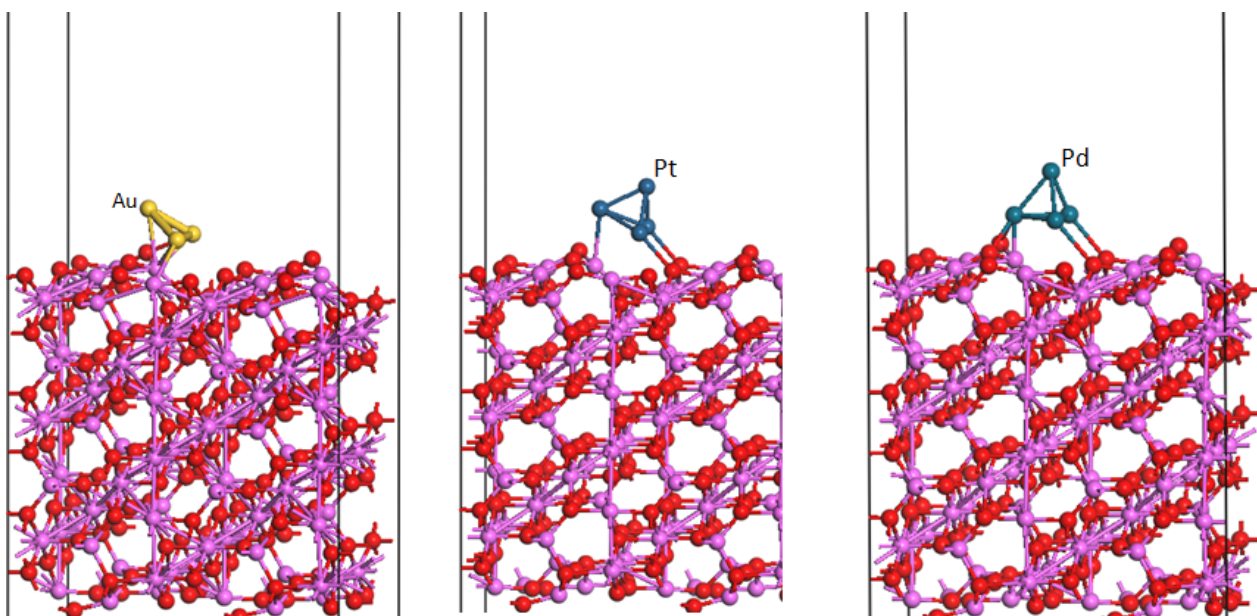


Fig. 3.  $\gamma$ -Alumina surface supported platinum, gold and palladium.

3.2. Effect of catalyst addition

Fig. 5 shows the catalytic degradation rate of butyl xanthate as a function of different amounts of added catalyst. The results in Fig. 5 suggest that the degradation rate of xanthate first increases and then decreases when the amount of added  $\gamma\text{-Al}_2\text{O}_3$  catalyst increased from 0.1 to 0.9 g/L. The highest degradation rate of xanthate is obtained at 0.5 g/L. It is clearly seen from the results that  $\gamma\text{-Al}_2\text{O}_3$  loaded with Pt still shows the best catalytic efficiency, and  $\gamma\text{-Al}_2\text{O}_3$  loaded with Pd displays the worst catalytic efficiency.

3.3. Effect of degradation time

Fig. 6 shows the effect of different degradation times on the degradation of butyl xanthate. The results suggest that

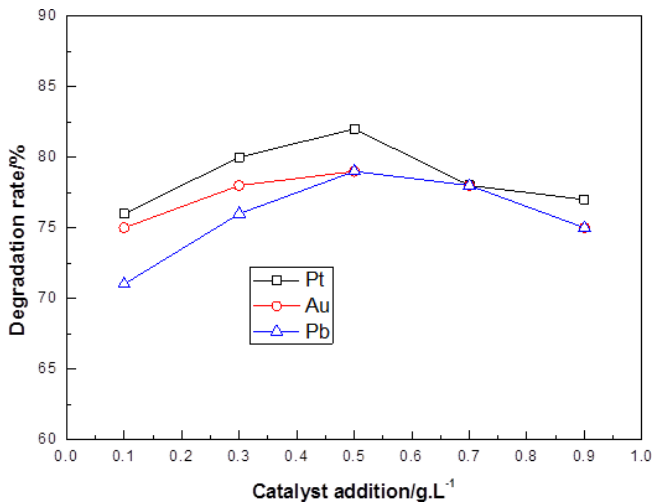


Fig. 5. Relationship between the amount of the different added catalysts and the degradation rate of butyl xanthate at 100 mg/L initial concentration of butyl xanthate, 1.75 g/h ozone flow and 5 min degradation time.

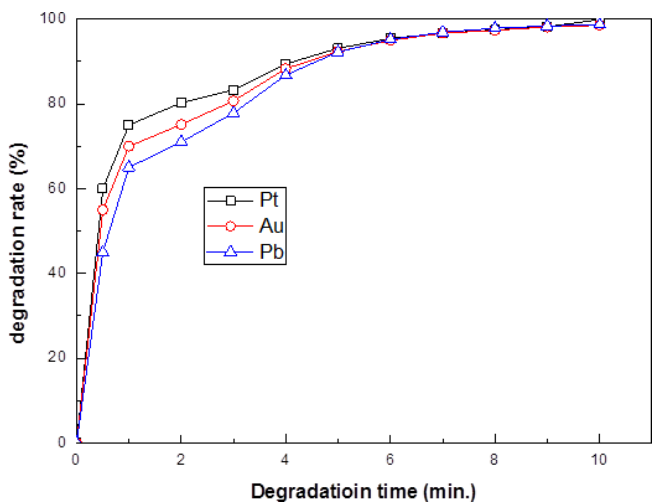


Fig. 6. Relationship between degradation time and degradation rate of butyl xanthate at the condition of 100 mg/L initial concentration of butyl xanthate, 1.75 g/h ozone flow and 0.5 g/L addition of catalyst.

the catalytic degradation process of butyl xanthate can be divided into three stages. The first stage is 0–1 min, in which the degradation rate is linear with time, and the degradation rate shows the highest increase with time. It is possible that the adsorption and degradation of  $\gamma\text{-Al}_2\text{O}_3$  occurred simultaneously. The second stage is 1–5 min, in which the degradation rate begins to increase less rapidly. The third stage is 5–10 min, in which the degradation rate begins to saturate and reaches the maximum value.

Comparison of the catalytic degradation rates for  $\gamma\text{-Al}_2\text{O}_3$  loaded with Pt, Au and Pd shows that Pt shows the fastest degradation during the period of 0–6 min, followed by Au and Pd. In addition, the catalytic degradation rates of butyl xanthate for Pt, Au and Pd metals are almost the same during the period of 6–9 min.

3.4. Effect of free radicals

The vitamin C (VC) reducing agent can eliminate a variety of oxidizing groups and is also an effective free radical scavenger that can suppress a variety of free radical chain reactions. To detect the presence or absence of  $\bullet\text{OH}$  during the oxidative degradation of butyl xanthate by heterogeneous ozone catalytic reaction, VC scavengers at different concentrations were added to the reaction solution. The effects of different VC concentrations on the degradation rate of xanthate are listed in Table 1 for the conditions of 0.5 g/L dose of Pt-supported  $\gamma\text{-Al}_2\text{O}_3$  catalyst, 1.75 g/h ozone flow and 10 min of degradation.

Table 1 shows that the degradation rate of xanthate in the absence of VC reaches 98.56%, and the increasing concentration of VC can obviously decrease the xanthate degradation rate, suggesting that there is a direct relationship between the inhibition of free radicals and the xanthate degradation. Hence, the catalytic degradation of xanthate proceeds by the mechanism of the oxidation of free radicals in the presence of Pt-loaded  $\gamma\text{-Al}_2\text{O}_3$ .

3.5. Product analysis of the degradation of xanthate

Ultraviolet scans of butyl xanthate samples with water at different degradation times were carried out in the xanthate solution with the initial concentration of 100 mg/L, 0.5 g/L Pt-loaded  $\gamma\text{-Al}_2\text{O}_3$  catalyst, and 1.75 g/h ozone flow. The results are shown in Fig. 7.

The wavelengths of the absorption peaks of the xanthate-related species are listed in Table 2. It is found from Fig. 7 that butyl xanthate has two strong characteristic absorption peaks at 226 and 301 nm. With increasing reaction time, the absorption peaks at 226 and 301 nm gradually decrease and

Table 1  
Effect of different VC concentrations on the degradation rate of butyl xanthate

VC concentration (mg/L)	Degradation rate (%)
0	98.56
100	89.03
250	78.15
300	66.79



even disappear, indicating that butyl xanthate was degraded. At the reaction time of 3 min, a new absorption peak appears at 223–224 nm, corresponding to the monothiocarbonate ion (ROCO<sub>2</sub><sup>-</sup>) and suggesting that the oxidation of the C=S bond has occurred. Moreover, the peak of 223 nm disappeared after 7 min, indicating that the monothiocarbonate was further oxidized. In addition, a new absorption peak appears at 208 nm after reaction for 3 min, corresponding to the absorption peak of CS<sub>2</sub> and indicating that the xanthate functional group (–CSS) is dissociated to form carbon disulfide. With

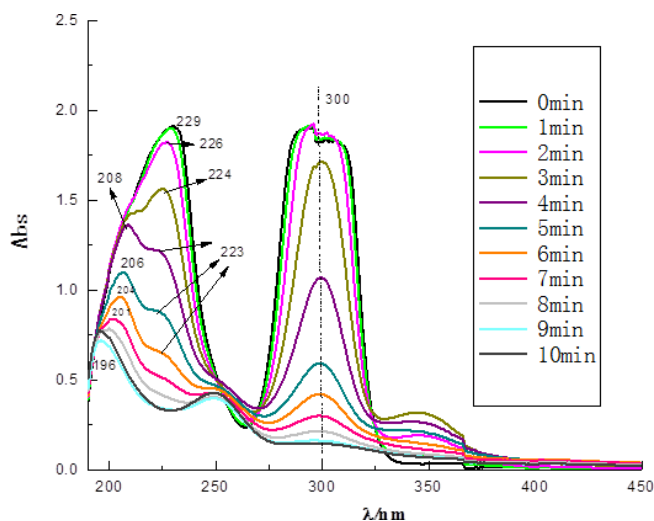


Fig. 7. UV spectra of the degradation of butyl xanthate by Pt-loaded  $\gamma$ -Al<sub>2</sub>O<sub>3</sub>.

Table 2

Wavelengths of the absorption peaks of species related to xanthate degradation

Species	Absorption peaks (nm)
Carbonyl, C=O	195
Carboxyl, –COOH	204
Carbon disulfide, CS <sub>2</sub>	206
Monothiocarbonate ion, ROCOS <sup>-</sup>	221–223
Dixanthaogen, ROCSS–SSCOR	238 or 283
Xanthic ion, ROCSS <sup>-</sup>	301 and 226

longer time, the peak at 208 nm shifts to 195 nm, corresponding to the carbonyl absorption peak, suggesting that carbon dioxide is the final degradation product of xanthate.

### 3.6. Adsorption of xanthate on metal-loaded $\gamma$ -Al<sub>2</sub>O<sub>3</sub> surfaces

Fig. 8 shows the adsorption structure of xanthate on the surface of  $\gamma$ -alumina loaded with Pt, Au and Pd. The adsorption energies are listed in Table 3. The adsorption energies of xanthate on the surfaces of Pt-, Au- and Pd-loaded  $\gamma$ -Al<sub>2</sub>O<sub>3</sub> are –194.87, –162.45 and –157.31 kJ/mol, respectively (Table 3), which is in agreement with their xanthate corresponding degradation rates. Hence, Pt-loaded  $\gamma$ -Al<sub>2</sub>O<sub>3</sub> has the best catalytic effect on the degradation of xanthate.

Table 4 shows the changes in the bond length for xanthate before and after the adsorption on the  $\gamma$ -Al<sub>2</sub>O<sub>3</sub> surface loaded with different metals, with the number of atoms shown in Fig. 2. The results in Table 4 show that the bond angle between two sulfur atoms becomes larger and the C–S single bonds (S1 and C1) are all significantly elongated from 1.675 to 1.765 Å (supported Pt surface), 1.735 Å (supported Au surface) and 1.745 Å (supported Pd surface). The bond length of the C=S (S2 and C1) double bond is also elongated, but the change is smaller than that of the C–S single bond. The distance between the O–C bond (C1 and O) is increased slightly, and the distance from C2 changes little.

Examination of the changes of the bond lengths in the xanthate molecule shows that the bond length change of xanthate adsorption on the Pt-loaded  $\gamma$ -Al<sub>2</sub>O<sub>3</sub> surface is the largest, followed by Au and Pd, which is consistent with the trend in the efficiency of xanthate degradation for these three catalysts. Hence, it is speculated that the degradation mechanism of xanthate catalyzed by Pt-, Au- and Pd-doped  $\gamma$ -alumina is related to the change of the bond length in the

Table 3

Adsorption energy of xanthate on  $\gamma$ -alumina surface loaded with different metals

$\gamma$ -Al <sub>2</sub> O <sub>3</sub> surface	Adsorption energy (kJ/mol)
Au loaded	–162.45
Pt loaded	–194.87
Pd loaded	–157.31

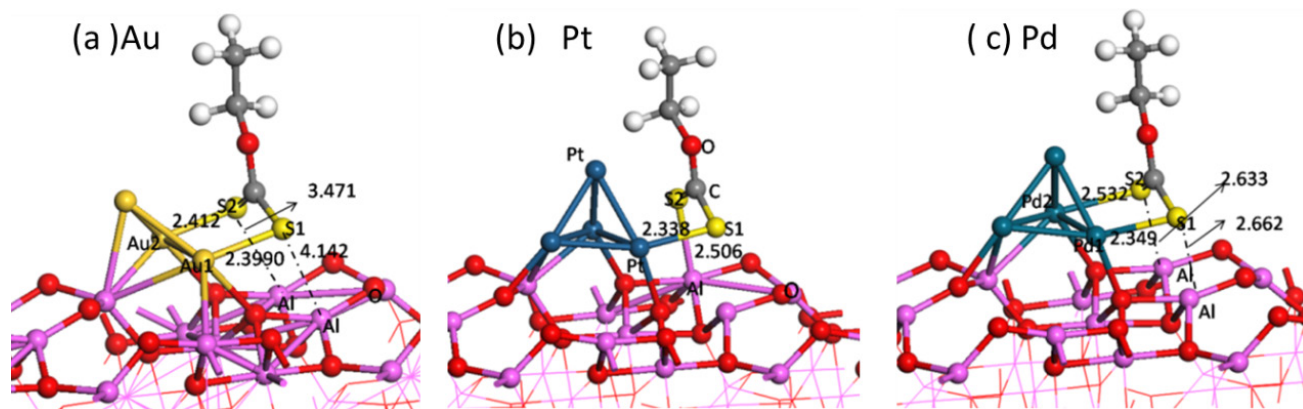
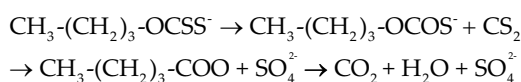


Fig. 8. Adsorption configuration of xanthate on  $\gamma$ -Al<sub>2</sub>O<sub>3</sub> surfaces loaded with Pt, Au and Pd.

Table 4  
Changes of bond lengths and angles in the xanthate molecule before and after adsorption

	Before adsorption (Å)	After adsorption (Å)		
		Pt-loaded surface	Au-loaded surface	Pd-loaded surface
S <sub>1</sub> -C <sub>1</sub>	1.675	1.765	1.735	1.745
S <sub>2</sub> -C <sub>1</sub>	1.676	1.732	1.718	1.703
C <sub>1</sub> -O	1.331	1.343	1.334	1.335
O-C <sub>2</sub>	1.466	1.460	1.463	1.465
∠S <sub>1</sub> C <sub>1</sub> S <sub>2</sub> (degree)	111.55	130.69	132.02	129.99

molecule, and the xanthate molecule will decompose starting with the weakest bond. Table 4 shows that the changes in the bond lengths of the S<sub>1</sub>-C<sub>1</sub> (single bond) and S<sub>2</sub>-C<sub>1</sub> (double bond) are the largest; hence, the degradation of xanthate most likely occurs through the oxidation of carbon and sulfur bonds. The ultraviolet spectrum suggests that xanthic ion (ROCSS) was oxidized to monothiocarbonate (ROCO<sub>2</sub><sup>-</sup>). The bond length of C-O shows a small change, indicating that it would take a long time to break, which is consistent with the appearance of the carbonyl products after the CS<sub>2</sub> in the UV spectrum. Based on the above results, the degradation path of butyl xanthate is speculated to be:



#### 4. Conclusions

The  $\gamma$ -Al<sub>2</sub>O<sub>3</sub> surfaces loaded with Pt, Au and Pd show an excellent catalytic effect on the degradation of butyl xanthate by heterogeneous ozone catalysis. In the initial degradation stage, Pt is the best, followed by Au and Pd, and the three metals show a similar effect on the degradation of xanthate in the final stage. The oxidation of free radicals is the mechanism of  $\gamma$ -Al<sub>2</sub>O<sub>3</sub> catalytic degradation of xanthate by the loaded precious metal. The degradation of xanthate begins with the oxidation of the carbon-sulfur bonds, followed by the breaking of the carbon-oxygen bonds, and finally by the degradation into small-molecule products such as carbon dioxide and sulfate.

#### References

- [1] X.P. Luo, M.H. Xie, Situation of purifying and comprehensive utilizing mineral processing wastewater and its development trend in nonferrous metal of emining, *China Min. Mag.*, 15 (2006) 51–56.
- [2] Y.K. Ou, *New Technology of Treatment of Wastewater from Pyrite Benefication by Ozone Oxidation and the Mechanism*, Central South University, Changsha, 2009.
- [3] F.H. Shi, J. Ma, Organics removal efficiency of ozonation and ozone catalytic oxidation process, *China Water Wastewater*, 20 (2004) 1–4.
- [4] K.L. Shao, J.T. Zhou, H. Lv, L.Y. Sun, Pesticide wastewater pretreatment by ozonation processes, *Chin. J. Environ. Eng.*, 3 (2009) 1259–1262.
- [5] R.P. Jia, Y.P. Chen, Current progress of ozone combined with other oxidation technique in wastewater treatment, *Ind. Water Treat.*, 27 (2007) 4–9.
- [6] C.T. Kresge, M.E. Leonowicz, W.J. Roth, J.C. Vartuli, J.S. Beck, Ordered mesoporous molecular sieves synthesized by a liquid-crystal template mechanism, *Nature*, 359 (1992) 710–712.
- [7] Y. Quan, A.X. Yin, C. Luo, L.D. Sun, Y.W. Zhang, W.T. Duan, H.C. Liu, C.H. Yan, Facile synthesis for ordered mesoporous  $\gamma$ -aluminas with high thermal stability, *J. Am. Chem. Soc.*, 130 (2008) 34–65.
- [8] M.M. Morris, P.F. Fulvio, M. Jaroniec, Ordered mesoporous alumina-supported metal oxides, *J. Am. Chem. Soc.*, 130 (2008) 15–21.
- [9] S.J. Clark, M.D. Segall, C.J. Pickard, P.J. Hasnip, M.I.J. Probert, K. Refson, M.C. Payne, First principles methods using CASTEP, *Z. Kristallogr.*, 220 (2005) 567–570.
- [10] M.D. Segall, P.J.D. Lindan, M.J. Probert, C.J. Pickard, P.J. Hasnip, S.J. Clark, M.C. Payne, First-principles simulation: ideas, illustrations and the CASTEP code, *J. Phys. Condens. Mat.*, 14 (2002) 2717–2744.
- [11] D. Vanderbilt, Soft self-consistent pseudopotentials in a generalized eigenvalue formalism, *Phys. Rev. B*, 41 (1990) 7892–7895.
- [12] H.J. Monkhorst, J.D. Pack, Special points for Brillouin-zone integrations, *Phys. Rev. B*, 13 (1976) 5188–5192.
- [13] J.D. Pack, H.J. Monkhorst, Special points for Brillouin-zone integrations – a reply, *Phys. Rev. B*, 16 (1977) 1748–1749.
- [14] V.G. Zavodinsky, M.A. Kuz'menko, A. Kiejna, Ab initio simulation of copper and silver adsorption on the MgO(111) surface, *Surf. Sci.*, 589 (2005) 114–119.